Journal of Chromatography A, 1517 (2017) 126–133

Contents lists available at ScienceDirect

Journal of Chromatography A

journal homepage: www.elsevier.com/locate/chroma

UV–vis degradation of α-tocopherol in a model system and in a cosmetic emulsion—Structural elucidation of photoproducts and toxicological consequences

Ségolène De Vaugelade[a,b], Edith Nicol[a], Svetlana Vujovic[a], Sophie Bourcier[a], Stéphane Pirnay[b], Stéphane Bouchonnet[a,*]

[a] Laboratoire de Chimie Moléculaire, Ecole Polytechnique, UMR-9168, 91128 Palaiseau Cedex, France
[b] EXPERTOX Laboratory, 14 rue Godefroy Cavaignac, 75011 Paris, France

ARTICLE INFO

Article history:
Received 18 June 2017
Received in revised form 27 July 2017
Accepted 5 August 2017
Available online 8 August 2017

ABSTRACT

The UV–vis photodegradation of α-tocopherol was investigated in a model system and in a cosmetic emulsion. Both gas chromatography coupled with tandem mass spectrometry (GC–MS/MS) and high performance liquid chromatography coupled with ultrahigh resolution Fourier transform ion cyclotron resonance mass spectrometry (LC-UHR-MS) were used for photoproducts structural identification. Nine photoproduct families were detected and identified based on their mass spectra and additional experiments with α-tocopherol-d_9; phototransformation mechanisms were postulated to rationalize their formation under irradiation. *In silico* QSAR (Quantitative Structure Activity Relationship) toxicity predictions were conducted with the Toxicity Estimation Software Tool (T.E.S.T.). Low oral rat LD50 values of 466.78 mg kg^{-1} and 467.9 mg kg^{-1} were predicted for some photoproducts, indicating a potential toxicity more than 10 times greater that of α-tocopherol (5742.54 mg kg^{-1}). *In vitro* assays on *Vibrio fischeri* bacteria showed that the global ecotoxicity of the α-tocopherol solution significantly increases with irradiation time. One identified product should contribute to this ecotoxicity enhancement since *in silico* estimations for *D. magna* provide a LC50 value 4 times lower than that of the parent molecule.

1. Introduction

Vitamin E is a well-known fat-soluble organic compound with high antioxidative properties, which protects against lipid peroxidation [1]. Vitamin E is a mixture of eight phenolic compounds, including four tocopherols (α, β, γ, δ) and four tocotrienols (α, β, γ, δ) [2]. They all include an amphiphilic structure containing a hydrophobic isoprenoid side chain and a hydrophilic chromanol ring [3]. All vegetables contain tocopherols; significant amounts are especially found in wheat, rice, corn and other seed germs, lettuce, soya and cottonseed oil [1]. On a biological point of view, the most active component of vitamin E is α-tocopherol [4], which is capable of capturing free radicals and quenching lipid peroxidation chain reactions. α-Tocopherol is a colorless to brown yellow, viscous oil that is insoluble in water. Because of its antioxidant activity, it is widely used as oil preservative and in pharmaceutical and cosmetic formulations like topical preparation, oral liquid preparation or emulsion, to prevent them from becoming rancid [1]. Vitamin E is often included in cosmetic skin creams and lotions to improve skin healing and reduce scarring. The toxicity of UV–vis light-induced compounds with environmental issues have been investigated intensily and is still widely studied today. A large number of vitamins are known to degrade through reactions photo-induced in the UV wavelength range [5,6]. This suggests that daylight could be highly destructive while artificial light has minimal influence on photosensitive vitamins because it normally provides negligible irradiation in the UV range [7]. Several kinds of mechanisms may be responsible for the photodegradation of vitamins. The photo-oxydation of Vitamin E in model systems and typical oil has been already reported but limited attention has been paid to structural eludidation and toxicity of photoproducts [8–16]. Psomiadou and Tsimidou reported pseudo-first order kinetics for α-tocopherol degradation in olive oil under fluorescent light [8,9]. First order kinetics were also described by Sabliov et al. as they studied the effects of temperature and UV light on the degradation of α-tocopherol in methanol and hexane [10]. Pirisi et al. showed that a solution of olive oil in hexane degraded with a rate constant (k) of 1.86×10^{-4} s^{-1} and a half-life of 112 min when irradiated with artificial light, and with a rate constant (k) of 1.03×10^{-4} s^{-1} and a half-life of 62 min when irradiated with sunlight [11]. The photol-

* Corresponding author.
E-mail address: stephane.bouchonnet@polytechnique.edu (S. Bouchonnet).

http://dx.doi.org/10.1016/j.chroma.2017.08.015
0021-9673/

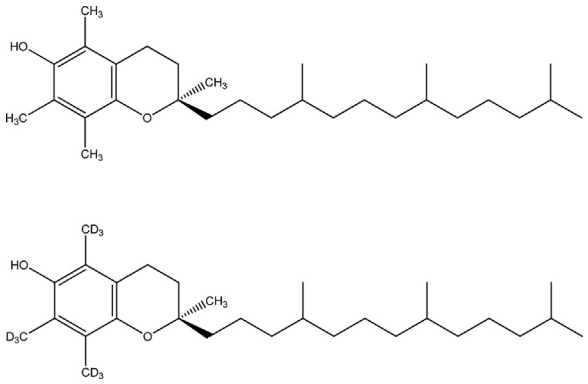

Fig. 1. Chemical structures of α-tocopherol and α-tocopherol-d_9.

ysis in liposomes by UVB rays was reported by Kramer and Liebler [12]. T. Miyazawa et al. reported a chemiluminescent product of α-tocopherol in methanol with methylene blue as photosensitizer [13]. G. W. Grams et al. have shown that α-tocopherol is susceptible to photooxidation in the presence of a dye sensitizer and that this oxidation in methanol leads to several compounds [14]. In an other study by Zhang et al., irradiation of α-tocopherol in acetonitrile led to the formation of the corresponding radical and cationic forms whereas only the radical species was observed after irradiation in methanol [15]. Finally, a study investigated the mechanisms of dimer and trimer formation from UVB-irradiated α-tocopherol [16].

The main objective of the present work was to characterize the photoproducts issued from direct photolysis of α-tocopherol. Solutions in acetonitrile were irradiated and analyzed by liquid-chromatography coupled with ultrahigh resolution tandem mass spectrometry (LC-UHR-MS/MS) and gas chromatography coupled with tandem mass spectrometry (GC–MS/MS). Twenty-seven photoproducts were detected. Ultra-high resolution measurements permited direct assignement of exact formulae while tandem experiments allowed structural elucidation for the major part of photoproducts. The second aim of this work was to analyse a personal care emulsion initally containing α-tocopherol as antioxydant, in order to investigate the presence of the photoproducts previously characterized in the model system. Finally, the potential toxicity of photoproducts was investigated *in silico* using QSAR calculations and *in vitro* using luminescence inhibition tests on *Vibrio fischeri* marine bacteria.

2. Experimental

2.1. Chemicals and reagents

DL-α-tocopherol (99.9% purity) was purchased from VWR (Fontenay sous Bois, France). α-tocopherol-d_9 (hydrogen atoms of methyl groups attached to the benzene ring are replaced by deuterium atoms, (see Fig. 1), 99% purity) was purchased from Avivagen Inc. (Chemaphor Service, Ottawa, Canada). Chromatographic grade solvents (99.99% purity), acetonitrile (ACN) and formic acid (FA), were purchased from Sigma Aldrich (St. Quentin Fallavier, France). A personal care emulsion containing 3000 mg L^{-1} of α-tocopherol as antioxidant agent was obtained from the cosmetic formulation laboratory Onyligne (La Neuville en Hez, France).

2.2. Sample preparation

Considering the poor water solubility of α-tocopherol in water (1.9×10^{-6} mg L^{-1} at 25 °C), α-tocopherol and α-tocopherol-d_9 solutions at 200 mg L^{-1} were prepared in acetonitrile in quartz tubes (2 mL), the solution was irradiated as soon as it was prepared. For the study devoted to the role played by dissolved oxygen in the photolysis process, a degassed solution was prepared in an inert atmosphere glove box (Vacuum Atmospheres Corps.). Argon was used as the inert gas. Pure α-tocopherol standard was kept under argon 24 h before preparation. O_2 and H_2O concentrations were less than 2 ppm. Air and water free acetonitrile was used for preparation. The quartz tube was filled and hermetically closed in a glove box before photolysis.

2.3. Sample extraction

The extraction process for cream samples of α-tocopherol and its photoproducts was conducted as follows: 1 g of the cosmetic emulsion was weighed into a plastic falcon tube, 10 mL of acetonitrile were added and the mixture was vortexed and immersed for 30 min in an ultrasonic bath heated at 60 °C to melt the lipidic phase and to facilitate the extraction of active components into acetonitrile. The tube was then centrifuged for 20 min at 3000 rpm. The supernatant was filtered using a 0.45 μm syringe filter (VWR, Fontenay sous Bois, France) before GC–MS and LC–MS analysis.

2.4. Photolysis experiments

Photolysis tests simulating UV–vis ray irradiation were carried out with a Q-SUN test chamber (Xe-1-B/S, Q-Lab Saarbücken, Germany) equipped with a xenon arc lamp (X-7640, Q-Lab Saarbücken, Germany). A natural light filter (X-7640, Q-Lab Saarbücken, Germany) has been used for a realistic reproduction of the full sunlight spectrum. The lamp power was 1800 W and the irradiation 0.68 W m^{-2} at a black-standard temperature of 55 °C. Irradiation control was maintained between 300 and 800 nm. For each experiment, 2 mL of a solution of α-tocopherol (see above) were used. To follow the evolution of photoproducts, experiments were carried out with 6 irradiation times ranging from 0 to 120 min: 0, 5, 10, 20, 30, 60 and 120 min.

2.5. GC–MS operating conditions

Analyses of standard and irradiated solutions were performed on a Varian® CP-3800 gas chromatograph equipped with a CP8400 autosampler and coupled with a Varian® Saturn 2000 mass spectrometer operated in the internal ionization mode. A CP-Sil 8 CB Low Bleed/MS capillary column, stationary phase composed of 5% diphenylsiloxane and 95% dimethylsiloxane (30 m x 0.25 mm i.d., 0.25 μm film thickness; Agilent, Waghäusel, Germany) was used. 1 μL of sample was automatically injected at 280 °C, in the splitless mode at a rate of 8 μL s^{-1}, with opening of the split valve after 1.5 min. High-purity helium (99.999%) was used as the carrier gas, and the flow was held constant at 1.4 mL min^{-1}. The initial oven temperature was held at 50 °C for 0.5 min, then raised up to 350 °C at 15 °C min^{-1} and hold at 350 °C for 15 min for a total acquisition time of 40.5 min. Ion-trap electrodes, manifold and transfer line were held at 200 °C, 100 °C and 280 °C, respectively. Ionization was performed by chemical ionization (CI) with methanol as reactant. Spectra were recorded using the automatic gain control (AGC) function with a target value of 5000. The filament emission current was set at 50 μA. The electron multiplier voltage was automatically optimized at 2200 V for a gain value of 10^5. Full scan mass spectra were acquired recording ions from m/z 50–500 at a frequency of 3 spectra s^{-1}. In multi-stage mass spectrometry (MS^n) experiments, precursor ions were stored with a Paul stability parameter (qz) of 0.30 and fragmented by collision-induced dissociation with activation energies ranging from 0.30 to 0.80 V in the resonant excitation mode.

2.6. LC–MS operating conditions

Chromatographic separation was carried out on a liquid chromatograph HPLC Alliance 2690 (Water Technologies, Saint-Quentin en Yvelines, France). For all experiments, 10 μL of sample were injected and separated on a C18 Pursuit-XRs Ultra 2.8 μm 50 mm x 2.0 mm column (Agilent Technologies, Les Ulis, France). Elution was performed using a 0.1 mL min^{-1} solvent flow with a mixture of solvents A (water, formic acid 0.1%) and B (methanol, formic acid 0.1%). Percentage of solvent B was increased from an initial value of 60% to 100% in 30 min and kept at 100% for 20 min. The gradient was then set at 60% of B for the last 10 min. For structural elucidation experiments, the HPLC system was coupled with an ultrahigh-resolution SolarixXR FT-ICR 9.4T mass spectrometer (Bruker Daltonics, Bremen, Germany). Ionization was achieved using electrospray in positive mode. Capillary and end plate voltages were set at −4.5 kV and −0.5 kV, respectively. Nitrogen was used as nebulizer and drying gas at 1 bar and 5 L min^{-1}, respectively, with a drying gas temperature of 300 °C. Ions were accumulated for 0.1 s in the collision cell. Time of flight was set up at 0.8 ms. Detection of ions in the ICR cell was set with a resolution of 4 Mpt (4×10^6 data points acquired) from *m/z* 57.74 to *m/z* 1000, with a 0.8389 transient duration in the broadband mode. One acquired scan was recorded for each spectrum, corresponding to MS or MS/MS duty cycles of approximately 1.03 s. In MS/MS experiments, the precursor ion was selected in the quadrupole with an isolation window of 1–2 Da and submitted to collision induced dissociation with collision energies of 0, 10 and 20 V. Elementary compositions of ions were determined using the DataAnalysis software with a 5 ppm tolerance.

2.7. In silico toxicity estimation

The Toxicity Estimation Software Tool (T.E.S.T.) has been developed by the U.S. Environmental Protection Agency to estimate toxicity using a variety of Quantitative Structure Activity Relationship (QSAR) mathematical models. Toxicity evaluations are based on the physical characteristics of a chemical structure (molecular descriptors). For example, the simple linear function of molecular descriptors (1) can be used to estimate the toxicity of chemicals.

$$\text{Toxicity} = ax_1 + bx_2 + c \quad (1)$$

where x_1 and x_2 are independent descriptor variables and *a*, *b*, and *c* are fitted parameters. The molecular weight and the octanol-water partition coefficient are examples of molecular descriptors [17]. For each endpoint, test set predictions showed that the so-called "consensus" method provided the best results. For example, in the *D. magna* module, consensus method achieved the best results in terms of both predictions accuracy and coverage; it has thus been retained for toxicity predictions. Toxicity values were estimated averaging the predicted toxicities from the above QSAR methods, in order to provide that the predictions were within the respective applicability domains.

2.8. In vitro bioassays

V. fischeri commercial *in vitro* test kits were used to evaluate the global ecotoxicity of the α-tocopherol solutions before and after several times of irradiation (0, 25, 50, 75, and 120 min). The freeze-dried luminescent bacteria and the luminometer were purchased from Hach Lange (Hach Lange GmbH, Düsseldorf, Germany). The experimental method used in this study is based on the ISO 11348-3 protocol (1998) [18]. Analysis were carried out at 15 °C. Lyophilized bacteria, previously frozen, were reconstituted just before analysis. Reconstitution was achieved by adding 1.3 mL of a saline solution provided by the manufacturer. The reconstituted solution had to be equilibrated for at least 15 min at 4 °C before testing. A working solution was prepared by adding 12.5 mL of dilution reagent to the hydrated bacteria. pH of solutions before and after irradiation were adjusted between 6.5 and 7.0 with sodium hydroxide and salinity was adjusted at 2% sodium chloride. Series of dilutions of test solutions were carried out in a 2% sodium chloride solution. Each dilution was tested in duplicate. Luminescence was measured before addition of the test solution and then after 5, 15 and 30 min and compared to the measured value of the bacterial control. The effective nominal concentration leading to 50% inhibition of bioluminescence after exposure for 5, 15 or 30 min was designated as the EC_{50} value. Two concentrations of α-tocopherol were used for the tested solutions, 150 and 200 μg mL^{-1}, depending on the expected EC_{50}.

3. Results and discussion

3.1. Photoproducts characterization

Irradiation of the acetonitrile solution of α-tocopherol led to the detection of 9 families of photoproducts. Mass spectra are too numerous to be all provided. The CID (collision induced dissociation) mass spectra of the protonated molecules corresponding to the major photoproducts are given in supplementary data files: SD-2 for PP7, SD-5 for PP1 and PP4. To make sure that none of them was formed without UV–vis irradiation, a non-irradiated solution (sampled at t0 has been systematically analyzed in GC–MS and LC–MS). No by-product was detected. Five groups of photoproducts, referred as PP1 to PP6, were detected by LC-HRMS and three photoproducts, referred as PP7 to PP9, were detected by GC–MS. The GC–MS and LC-HRMS chromatograms recorded for an irradiation time of two hours are given in the supplementary data files SD-1 and SD-2; kinetic data are reported in SD-3. Table 1 reports the retention times, the *m/z* ratios of MH^+ ions, the main transitions issued from CID experiments and the number of deuterium atoms present in each compound when irradiation is carried out on α-tocopherol-d_9. Elementary formulae were determined with a tolerance of 5 ppm. The results in Table 1 show that the photodegradation process begins via oxidation of α-tocopherol through oxygen addition onto it. The solubility of oxygen in acetonitrile is high enough (8.1 versus 1.0 mM in water under standard temperature and pressure conditions) to permit such a mechanism [19]. According to literature results, O_2 addition onto a 6-membered-ring – fully conjugated or including at least a double bond – may occur via three mechanisms: concerted 1,2-cycloaddition, concerted 1,4-cycloaddition and ene reaction of singlet oxygen onto a double bond. The predominant role of dissolved O_2 was confirmed by analyzing a solution of α-tocopherol previously degassed (see the experimental part), for which the initial amount of α-tocopherol is still measured after two hours of irradiation.

3.1.1. PP-1-1 to PP1-6

1,2-cycloaddition on α-tocopherol may lead to the six dioxetane structures referred as **A** to **F** in Fig. 2. These structures are expected to be unstable: the dioxetane ring should open through a concerted mechanism, as shown by Barlett et al. for the photoxidation of dihydropyrane [20]. The six products corresponding to $C_{29}H_{50}O_4$ (*m/z* 463.3796 for MH^+), eluted between 38.49 and 43.85 min, are assumed to result from 1,2-cycloaddition of O_2 on α-tocopherol, followed by opening of the four-membered ring, to lead to keto and carboxylic functions in all cases, at the exception of structure **E**, whose opening leads to a ten-membered ring. In MS/MS experiments, all the corresponding MH^+ ions undergo successive losses of water and carbon monoxide (transitions *m/z* 463.3767 → *m/z*

Table 1
Analytical results related to the LC–MS and GC–MS detection of tocopherol photoproducts.

Compound	Retention time (min)	m/z of MH^+	Ion raw formula	m/z shift for Tocopherol-d_9	Main transitions in MS/MS (m/z)	Chemical structure
LC–MS data (ESI+ high resolution)						
PP1-1 to PP1-6	38.49–43.85	463,37967	$C_{29}H_{51}O_4^+$	+ 9 445.36612 → 417.37141[1]	463.37675 → 445.36612	Tocopherol + O_2
PP2	39.12	409.33197	$C_{25}H_{45}O_4^+$	+ 3	409.33031 → 391.34074	Tocopherol + O_2 — C_4H_6
PP3-1 to PP3-3	34.62–42.17	407.35291	$C_{26}H_{47}O_3^+$	+ 6 389.34076 → 361.34598	407.31225 → 389.34076	Tocopherol + O_2 — C_3H_4O
PP4-1 to PP4-10	39.70–47.10	445.36931	$C_{29}H_{49}O_3^+$	+ 9 445.36634 → 417.37110 427.35631 → 409.34528 427.35631 → 399.36067	445.36634 → 427.35631	Tocopherol+ O − 2H
PP5-1 and PP5-2	42.21–47.11	427.35933	$C_{29}H_{47}O_2^+$	+ 8 427.35933 → 399.36088 427.35933 → 385.17716	427.35933 → 409.32995	Tocopherol- 4H
PP6-1 and PP6-2	45.08–45.55	419.35363	$C_{27}H_{47}O_3^+$	+ 6 153.05429 → 125.05352	419.35077 → 153.05429	Tocopherol + O_2 - C_2H_4O
GC–MS data (CI+ low resolution)						
PP7	15.05	269		0 269 → 125 269 → 111 111 → 83	269 → 139	$C_{18}H_{36}O$
PP8	18.38	325		0 307 → 289 325 → 269	325 → 307	$C_{21}H_{40}O_2$
PP9	19.31	391		+ 6	391 → 125	$C_{25}H_{42}O_3$

[1] Not observed in the case of PP1-6.

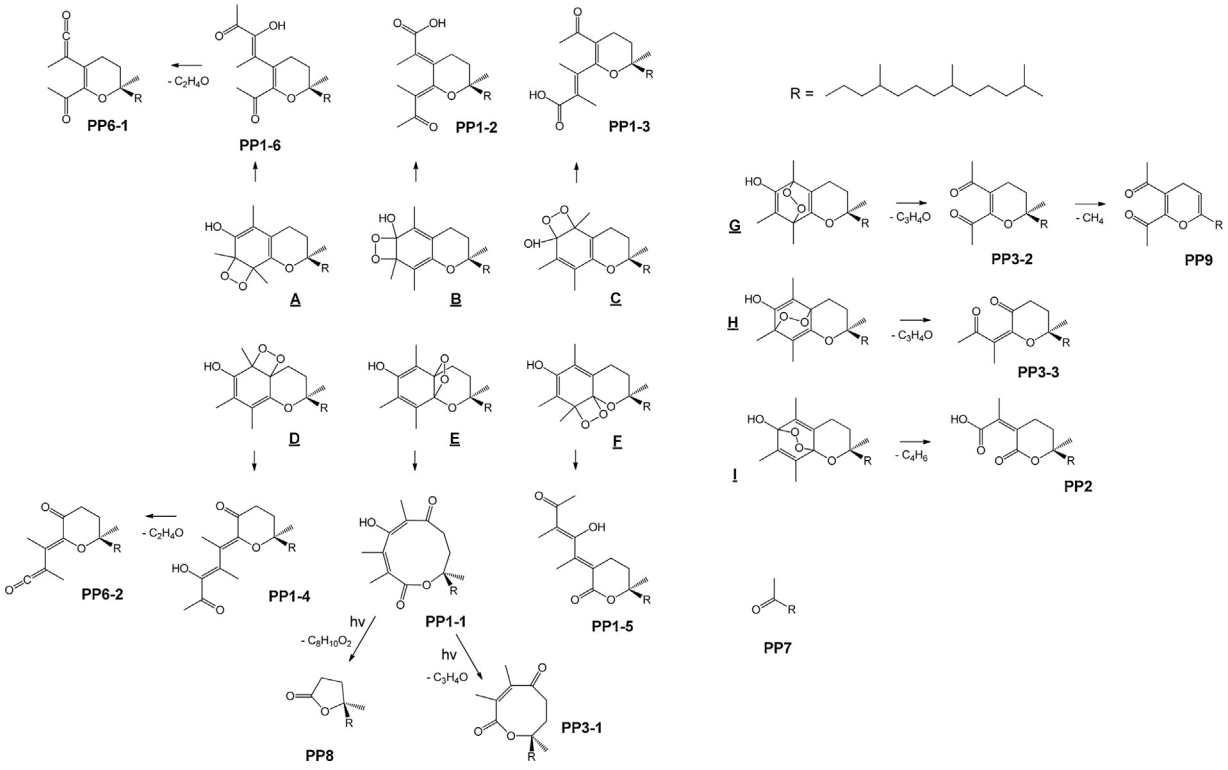

Fig. 2. Chemical structures and postulated mechanisms for the formation of photoproducts PP1-1 to PP1-6, PP2, PP3-1 to PP3-3, PP6-1, PP6-2, PP7, PP8 and PP9.

445.3661 → m/z 417.3714). H_2O is also eliminated from the deuterated analogues, meaning that water is eliminated after protonation of a hydroxyl group. Only water loss is observed in the case of PP1-6. This is in agreement with the suggested structures that may all lose water and carbon monoxide with the exception of PP1-6 for which only water elimination is possible. PP1-6 may thus be attributed to the last eluting isomer while PP1-1 could correspond to the first one based on its small cross section in comparison with other compounds. Other isomers cannot be attributed to chromatographic peaks on the basis on MS/MS results nor chromatographic considerations. Examples of the mechanism postulated for PP1 formation are supplied in supplementary data file SD-4.

3.1.2. PP2

PP2 corresponds to $C_{25}H_{44}O_4$ (m/z 409.33199 for MH^+); it elutes at 39.12 min. It is assumed to result from 1,4-addition of O_2 onto α-tocopherol (structure **I** in Fig. 2), followed by C_4H_6 elimination (C_4D_6 with α-tocopherol-d_9) according to the mechanism described in SD-4. The only transition observed in MS/MS experi-

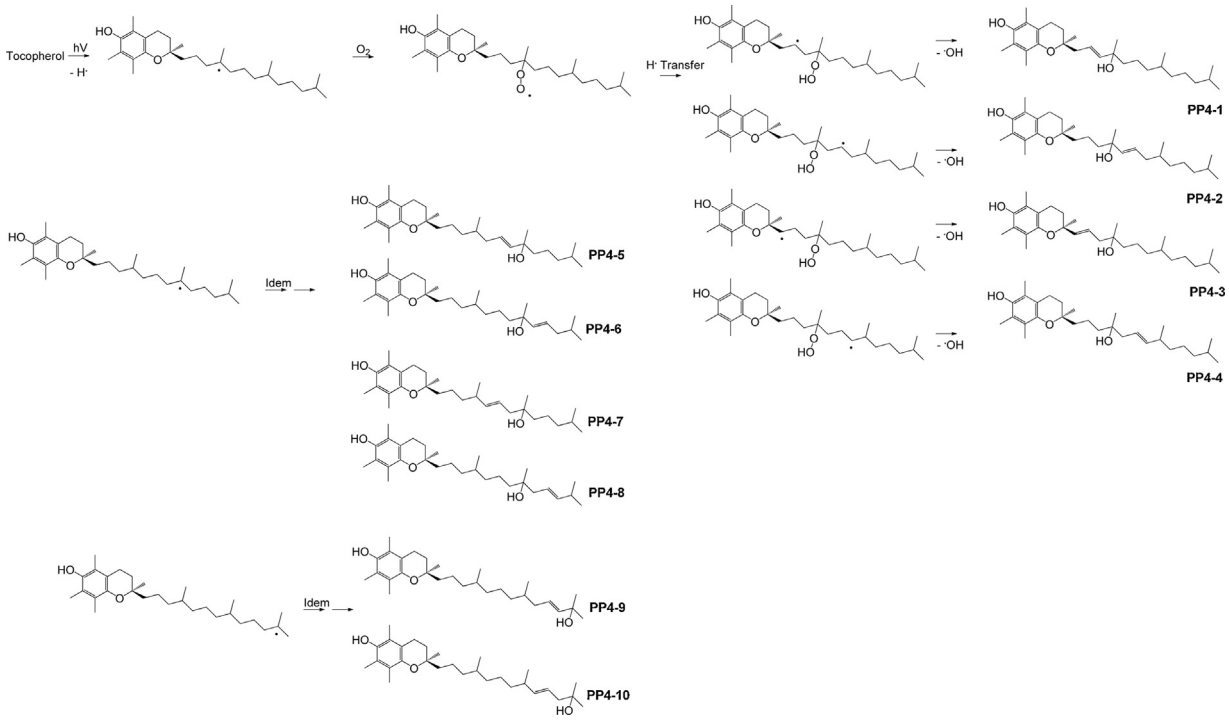

Fig. 3. Chemical structures and postulated mechanisms for the formation of photoproducts PP4-1 to PP4-10.

ments corresponds to the loss of water from $PP2H^+$, in agreement with the postulated structure.

3.1.3. PP3-1 to PP3-3

Three products corresponding to $C_{26}H_{46}O_3$ (m/z 407.35291 for MH^+) are eluted between 39.62 and 42.17 min. Two of them are also assumed to result from 1,4-addition of O_2 onto α-tocopherol (structures **G** and **H** in Fig. 2). By the same mechanism that for the opening of **I**, the dissociation pathways of **G** and **H** consist in CH_3CCOH eliminations (CD_3CCOH) with α-tocopherol-d_9) to provide PP3-2 and PP3-3. PP3-1 was assumed to result from CH_3CCOH elimination from PP1-1 after irradiation of the later (see Fig. 2). The resulting cyclic structure is in agreement with a compound eluting before PP3-2 and PP3-3. In MS/MS experiments, the corresponding MH^+ ions all undergo loss of water; carbon monoxide is also eliminated in the case of PP3-1 and PP3-2, in accordance with the proposed structures.

3.1.4. PP4-1 to PP4-10

PP4-1 to PP4-10 isomers have a raw formula ($C_{29}H_{48}O_3$) resulting from oxygen addition and elimination of two hydrogen atoms from α-tocopherol. Their retention times – ranging from 39.70 to 47.10 min – are shorter than that of α-tocopherol (50.16 min) and suggest that the six-membered ring has been kept during photolysis. Under collisional activation, the pseudomolecular ion undergoes loss of CO and successive elimination of two water molecules, indicating that a hydroxyl group was added to the initial structure. Water elimination after O_2 addition was first postulated but none of the structures resulting from 1,2- or 1,4-addition on the aromatic ring (i.e. A–I in Fig. 2) allows the elimination of water. Irradiation of α-tocopherol-d_9 also led to elimination of two hydrogen atoms and creation of a new unsaturation, meaning that hydroxyl addition occurred on the aliphatic chain, as well as H_2 elimination. The mechanisms postulated on Fig. 3 all begin by photo removal of a hydrogen atom from a carbon atom bound to at least one methyl group, leading to a tertiary radical. After O_2 addition, concerted hydrogen transfer and radical hydroxyl elimination lead to ten structures, in agreement with the ten coeluted photoproducts detected on the chromatogram between 39 and 47 min (SD-1).

3.1.5. PP5-1 and PP5-2

Photoproducts PP5-1 and PP5-2, corresponding to $C_{29}H_{47}O_2$ (m/z 427.3593 for MH^+) are eluted at 42.21 min and 47.11 min. They have lost four hydrogen atoms in comparison with α-tocopherol. The deuterated analogue losses one deuterium atom and three hydrogen atoms under irradiation, suggesting the elimination of one hydrogen from one methyl group, one from the hydroxyl function and two from the six-membered ring. A mechanism beginning by hydrogen atom removal from the hydroxyl group has been postulated (see Fig. 4). This $\dot{H}$ elimination is followed by another one ($\dot{D}$ in the case of deuterated analogue) and by a concerted H_2 loss to increase conjugation of the system. Both losses of H_2O (after protonation of the ether function and hydride transfer from the aliphatic chain) and CO (following protonation on the ring carrying the keto group) under collisional activation are in agreement with the postulated structures. Elimination of $CH_2C{=}CHCH_3$ (M = 42) may be rationalized by the loss of the end of the aliphatic chain.

3.1.6. PP-6-1 and PP6-2

Two isomeric compounds, referred as PP6-1 and PP6-2, corresponding to $C_{27}H_{46}O_3$ (m/z 419.3536 for MH^+) are eluted at 45.08 min and 45.55 min. They are assumed to result from acetaldehyde loss from PP1-6 and PP1-4 (they can also be rationalized in terms of simultaneous eliminations of methane and carbon monoxide). The loss of $HCOCH_3$ was replaced by that of $HCOCD_3$ in experiments with deuterated α-tocopherol, indicating elimination of three hydrogen atoms from a methyl group and one hydrogen atom initially bound to the oxygen atom of the hydroxyl group or to a sp3 carbon of the six-membered ring. Based on these results, PP1-6 and PP1-4 are, among PP1-1 to PP1-6, the only structures for which $HCOCD_3$ loss from the deuterated analogue is possible. This acetaldehyde elimination is assumed to occur through a concerted four-membered mechanism that is given in supplementary

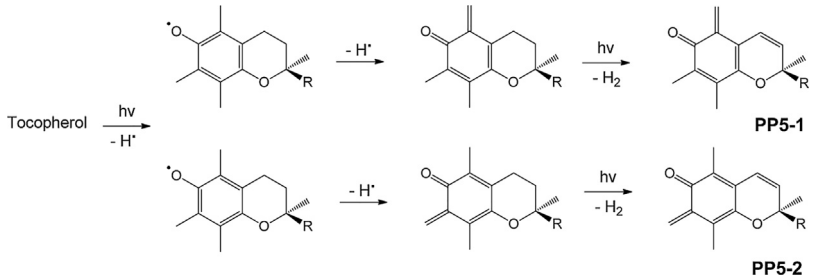

Fig. 4. Chemical structures and postulated mechanisms for the formation of photoproducts PP5-1 and PP5-2.

data SD-4. The structures proposed on Fig. 2 for PP6-1 and PP6-2 are in agreement with the results of CID experiments performed on the protonated molecules that show consecutive eliminations of $C_{19}H_{39}$ and carbon monoxide.

3.1.7. PP7

In GC–MS coupling, one product corresponding to *m*/*z* 269 for MH^+ is eluted at 15.05 min. The absence of shift for the deuterated photoproduct means that all deuterium have been removed during the phototransformation process. In MS/MS experiments, the characteristic profile of an n-alkane spectrum, regularly-spaced of alkyl groups $(C_nH_{2n+1})^+$ is an indication of the presence of the aliphatic chain (*m*/*z* 225). The structure proposed for PP7 is the ketone resulting from opening of the tetrahydropyran. The transitions observed in CID experiments correspond to fragmentations of the alkyl chain.

3.1.8. PP8

PP8 corresponding to *m*/*z* 325 for MH^+ is eluted at 18.38 min in GC–MS. It was assumed to result from opening of PP1-1 (see Fig. 2) through a Norish-type photoinduced reaction followed by cyclization into a five-membered ring. The lactone structure proposed is coherent with the loss of all the deuterated atoms for the deuterated analogue and with the MS/MS dissociation pathways displayed in the supplementary data file SD-6.

3.1.9. PP9

One product corresponding to *m*/*z* 391 for MH^+ is eluted at 19.31 min in GC–MS. The deuterated analogue of PP9 has kept six deuterium atoms meaning that a methyl group was eliminated during photoformation of this compound. The PP9 structure displayed in Fig. 2, postulated on the basis of the main MS/MS transition observed from $PP9H^+$ (see the supplementary data file SD-6) is easy to form from PP3-2, through concerted methane elimination to provide a more conjugated thus more stable species.

F.Pirisi et al. studied the photodegradation of α-tocopherol in olive oil, hexane, anhydrous n-hexane, and triolein. A main product identified by ^1H and ^{13}C NMR and GC–MS as 5-formyl tocopherol produced by Michael addition of H_2O was found in the non-anhydrous hexane model system [11]. T. Miyazawa et al. reported the formation of 8a-hydroperoxy-α-tocopherone, which has been characterized by ^1H NMR and FAB-MS [13]. G. W. Grams et al. showed that α-tocopherol is susceptible to photooxidation in the presence of a dye sensitizer leading in methanol to several compounds including α-tocoquinone 2,3-oxide [14]. Kramer et al. described the UVB induced photooxydation of α-tocopherol in liposomes and in an acetonitrile/H_2O (4:1 v/v) solution. Oxidation products, including a quinone, epoxyquinones, dimers and epoxytocopherones, were initially separated by HPLC; their UV spectra and retentions times were compared to those of standards. In GC–MS, full-scan mass spectra and GC retention times were also used to confirm the formation of epoxyquinones. Dimers were analyzed by LC–APCI–MS. A more recent work reported the photochemical formation of α-tocopherol dimers and trimers after UV-irradiation of α-tocopherol in a thin film obtained by the solvent evaporation of a concentrated (2153 μg mL^{-1}) α-tocopherol solution. After HPLC separation, dihydroxydimer, spiromer and trimers were analyzed by APCI-MS or ESI–MS and compared to MS-MS analysis of authentic standards [16]. None of these photoproducts were detected in the present study. Concerning dimers and trimers, it may be due to the low concentration used, which likely does not permit intermolecular reactions. Concerning other species, these differences may be attributed to the differences in irradiated media since photochemical reactions are known to be very matrix-dependent.

3.2. Real sample analysis

In recent years, the photostabilities of topical formulations were investigated, especially those of sunscreens, to assure their performance on human skin. Many formulations contain vitamins to ensure the hydration and anti-aging effects on the skin. Vitamin A, C and E are frequently added. According to Gaspar et al., formulations containing combinations of vitamins are more suitable in deeper layers hydration and anti-aging effects. Addition of UV-filters is interesting in combination with vitamins for the reduction of skin irritation due to vitamin A conversion into tretinoin [21]. Guaratini et al. study has shown that addition of vitamins to the basic formulation affected the formulation physical integrity and concludes on the necessity to study both physical aspect and chemical degradation [22]. The light-induced transformation of α-tocopherol in the real sample (initially containing 3000 μg/mL of α-tocopherol) was investigated with the photolysis conditions used for the standard solution. According to both GC–MS and LC–MS results, the initial amount of α-tocopherol decreases by about 50% after 2 h of irradiation. Only two isomers of PP1, five isomers of PP4 and PP7 were detected after 2 h of irradiation. The photoproducts found in the reference emulsion correspond to the major ones detected by both GC–MS and LC–MS in the irradiated standard solution. Consequently, it is impossible to state if the other photoproducts were not detected because they had not been formed (or in trace amount) or because they are present at concentrations below the analytical detection thresholds, which are expected to be likely elevated due to matrix effects.

3.3. Toxicity predication

3.3.1. In silico toxicity estimation

Table 2 reports the predictive values for oral rat LD50, *Daphnia magna* LC50 (48 h), and the predictive conclusions on the developmental toxicity for the photoproducts of α-tocopherol. Oral LD50 and *Daphnia magna* LC50 of PP6-1 and PP6-2, which contain a ketene functional group, were not calculated by the software T.E.S.T. since it had no sufficient parameters for the corresponding structures. Oral rat LD50 indicates the amount of chemical in $mg.kg^{-1}$ body weight (bw) that would cause 50% of a test population of rats to die after oral administration. As vitamin E

Table 2
In silico toxicity predictions provided by the software T.E.S.T. for the photoproducts of tocopherol.

ID	Oral rat LD50 (mg/kg)	Developmental toxicity	Daphnia magna LC50 48 hours (mg/L)
α-tocopherol	5742.54	Toxicant	0.22
PP1-1	1211.76	Toxicant	0.54
PP1-2	3695.21	Toxicant	0.27
PP1-3	1548.23	Toxicant	0.38
PP1-4	1344.37	Toxicant	0.56
PP1-5	2886.81	Toxicant	0.36
PP1-6	2341.34	Toxicant	0.71
PP2	1949.42	Toxicant	0.92
PP3-1	4383.53	Toxicant	0.46
PP3-2	1255.43	Toxicant	0.54
PP3-3	1869.9	Toxicant	0.42
PP4-1	2520.64	Toxicant	0.23
PP4-2	1558.59	Toxicant	0.22
PP4-3	1584.71	Toxicant	0.22
PP4-4	2039.75	Toxicant	0.33
PP4-5	1044.31	Toxicant	0.35
PP4-6	2692.95	Toxicant	0.79
PP4-7	1622.2	Toxicant	0.36
PP4-8	1519.56	Toxicant	0.41
PP4-9	1374.95	Toxicant	0.35
PP4-10	1290.38	Toxicant	0.83
PP5-1	466.78	Toxicant	0.0551
PP5-2	467.9	Toxicant	0.15
PP6-1	NC[a]	Toxicant	NC
PP6-2	NC	Toxicant	NC
PP7	4120.22	Non-toxicant	1.54
PP8	3752.7	Non-toxicant	0.47
PP9	2549.1	Toxicant	0.43

[a] NC: Not calculated, because of insufficient parametrization.

is prescribed as a nutritional complement, the question of the safety of oral administration had been previously examined. The acute, subacute, subchronic and chronic toxicity, mutagenicity and reproductive toxicity of various derivatives of α-tocopherol, e.g. α-tocopheryl acetate, have been investigated using *in vivo* approaches [23]. Wheldon et al. fed all-rac-α-tocopheryl acetate to rats in daily doses of 500, 1000 and 2000 mg kg^{-1} bw for 104 weeks. No significant effects on clinical-chemical parameters have been reported. Slight effects on liver weights and small increase of liver enzymes in serum have been observed. Hemorrhages were observed at the highest doses, in male rats only. The tumor rate also showed no difference from control animals, with the exception of decrease of mammary tumors. The acute oral rat LD_{50} has not been determined but it has been reported that α-tocopherol was tolerated at doses up to 5000 mg kg^{-1} bw in rats [24]. This is in accordance with the predicted value of 5742.54 mg kg^{-1} provided by the simulation program used in the present study.

The consensus method for oral rat LD50 provided low predicted values of 466.78 mg kg^{-1} and 467.90 mg kg^{-1} for PP5-1 and PP5-2, respectively. According to the Hodge and Sterner toxicity classification scale, these values correspond to a moderate toxicity compared to a practically non-toxic class for parent compound and a slight toxicity class for all other photoproducts (between 1044.31 mg kg^{-1} for PP4-5 and 4120.22 mg kg^{-1} for PP7). This higher toxicity in comparison with that of the parent molecule was also observed with the *Daphnia magna* LC50 (48 h) estimation in the cases of PP5-1 and PP5-2 with LC50 values of 0.055 mg L^{-1} and 0.15 mg L^{-1}, respectively. The relationship between the ring number and the aquatic toxicity has been reported by Black et al. for three chemical aromatic hydrocarbon classes [25]. No mutagenicity effect has been reported in literature for α-tocopherol. A negative mutagenicity has been predicted for α-tocopherol in the present study. This is coherent with the absence of induction of chromosomal damage or the absence of increase in the sister chromatid exchange rates reported by Gebhart et al. who tested the

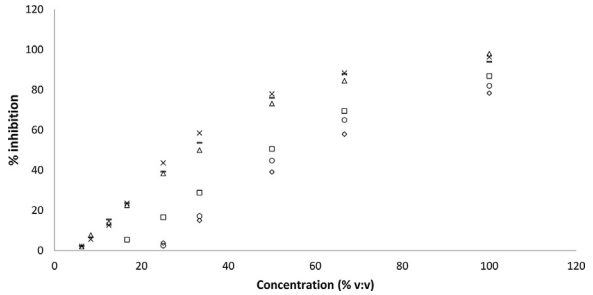

Fig. 5. Response-dose curves for the reference and irradiated solutions of α-tocopherol solutions with the *Vibrio fischeri* bioluminescence inhibition test.

mutagenicity in human lymphocytes *in vitro* [26]. No mutagenicity effect has been predicted for the photoproducts. The potential development toxicity of α-tocopherol and its photoproducts has also been investigated. Results of simulation tests show that α-tocopherol could be responsible for developmental toxicity. Some studies dedicated to the teratogenicity and reproductive toxicity of vitamin E reported a teratogenic effect while others studies disproved it. Studies on animal experiments have shown that vitamin E deficiency was responsible of teratogenic effects. A study on mice showed some malformations (exencephaly, open eye, and micrognathia) on a total of 91 offsprings from 7 litters from treated animals (daily doses of 591 mg α-tocopherol by gavage on days 7–11 of pregnancy) [27]. In a study reported in the Catalog of Teratogenic Agents, vitamin E was administered in amounts of 150 or 300 mg kg^{-1} day^{-1} to pregnant mice on days 6, 8 and 10 of gestation [28]. Growth retardation and fetal survival were increased in the treated group. The incidence on cleft palate was also increased. Studies on rat (75 mg day^{-1}) were negative. Other studies have shown a higher rate of exencephaly, hydrocephalus, and cleft palate in the litters of rats and mice after administration of high doses of vitamin E [29,30]. However, other animal investigations did not find teratogenic effect of vitamin E [31]. According to the results of the present studies, all the photoproducts at the exception of PP7 and PP8 could be also responsible for development toxicity, but it is difficult to conclude on the potential development toxicity of α-tocopherol considering the conclusions of previous published studies.

3.3.2. *In vitro* bioassays

The objective of the ecotoxicity tests carried out on *Vibrio fischeri* was to evaluate the consequences of UV–vis irradiation on the toxicity of reference solutions and irradiated solutions by comparing their EC_{50}. A solution of α-tocopherol at 3000 mg L^{-1} in acetonitrile was irradiated for 0 (reference solution), 25, 50, 75, 100 and 120 min. Samples were then diluted in water so that tests were conducted on aqueous mixtures with less than 20% acetonitrile. For each sampling time, two "final" concentrations were tested: 150 and 200 mg L^{-1}. Fig. 5 displays the inhibition percentage of *Vibrio fischeri* bioluminescence after 5 min of incubation as a function of the ratio (v:v) of the tested solution in mixture with the bacteria solution. EC_{50} on *Vibrio fischeri* were measured with three incubation times (5, 15 and 30 min) and are reported in the supplementary data file SD-7. Measurements carried out at 50% v:v in the bacteria solution show that the solution irradiated for 100 min leads to an inhibition percentage twice that of the reference solution. Toxicity increases up to 100 min of photolysis and remains stable after this time, which corresponds to total degradation of α-tocopherol. A slight difference is noted between the EC_{50} determined at 5, 15 and 30 min, which can be interpreted in terms of chronic toxicity.

4. Conclusion

In the present study, the photodegradation of α-tocopherol under UV–vis irradiation led to the formation of nine photoproduct families. Six main transformation products were separated and identified using LC-HR-MS/MS while three minor ones were characterized by GC–MS. Different photoreaction mechanisms had to be involved to rationalize the formation of all of them. In many cases, the photodegradation process of α-tocopherol begins via oxidation of α-tocopherol through oxygen addition onto the aromatic six-membered ring. PP1 and PP6 isomers result from O_2 1,2-cycloaddition onto the aromatic ring followed by ring-opening, while PP2, PP3-2, PP3-3 result from 1,4-cycloaddition of O_2 onto the same ring, followed by C_4H_6 and C_3H_4O eliminations. It has been shown that O_2 addition may also occur on the aliphatic chain. Concerted hydrogen transfer and radical hydroxyl elimination following this addition led to the formation of the ten PP4 isomers. PP5 formation begins by the elimination of the hydrogen atom carried by the hydroxyl group, leading to the well know α-tocopheryl radical through photoinduced direct cleavage, and consecutive hydrogen eliminations from methyl groups, and from the non-aromatic six-membered ring. Finally, ketone PP7 results from opening of the tetrahydropyran and PP8 results from opening of PP1-1 through a Norish-type photoinduced reaction. In the present work, a real cosmetic emulsion containing α-tocopherol as antioxydant agent was submitted to irradiation under laboratory conditions. Some PP6 and PP4 photoproducts were detected, demonstrating the suitability of the methodology to investigate the phototransformation of regulated cosmetic raw material, and detect their potentially hazardous by-products in complex matrices like personal care product. The results of *in vitro* assays on *Vibrio fischeri* bacteria showed that the global ecotoxicity of the α-tocopherol solution significantly increases with irradiation time. PP5-1 should likely contribute to this ecotoxicity enhancement since *in silico* estimations for *D. magna* provide a LC50 value 4 times lower than that of the parent molecule.

Appendix A. Supplementary data

Supplementary data associated with this article can be found, in the online version, at http://dx.doi.org/10.1016/j.chroma.2017.08.015.

References

[1] M. Waghmode, M. Kamble, A. Shruti, Pharmaceutical profile of alpha-tocopherol –A brief review, Int. J. Pharm. Chem. Biol. Sci. 1 (3) (2012) 1023–1039.
[2] M.G. Traber, Utilization of vitamin E, Biofactors 10 (1999) 115–120.
[3] R. Ricciarelli, J.M. Zingg, A. Azzi, The 80th anniversary of vitamin E: beyong its antioxidant properties, Biol. Chem. 383 (3-4) (2002) 457–465.
[4] G.W. Burton, K.U. Ingold, Vitamine E: application of the principles of physical organic chemistry to the exploration of its structure and function, Acc. Chem. Res. 19 (7) (1986) 194–201.
[5] M.C. Allwood, J.H. Plane, The wavelength-dependent degradation of Vitamin A exposed to ultraviolet radiation, Int. J. Pharm. 31 (1986) 1–7.
[6] M.C. Allwood, J.H. Plane, The degradation of vitamin A exposed to ultraviolet radiation, Int. J. Pharm. 19 (1984) 207–213.
[7] M.C. Allwood, The influence of light on vitamin A degradation during administration, Clin. Nutr. 1 (1982) 63–70.
[8] E. Psomiadou, M. Tsimidou, Stability of virgin olive oil. 1. Autoxydation studies, J. Agric. Food. Chem. 50 (2002) 716–721.
[9] E. Psomiadou, M. Tsimidou, Stability of virgin olive oil. 2. Photo-oxydation studies, J. Agric. Food. Chem. 50 (2002) 722–727.
[10] C.M. Sabliov, C. Fronczek, C.E. Astete, M. Khachaturyan, L. Khachaturyan, C. Leonardi, Effect of temperature and UV light on degradation of α-tocopherol in free and dissolved form, J. Am. Oil Chem. Soc. 86 (2009) 895–902.
[11] F.M. Pirisi, A. Angioni, G. Bandino, P. Cabras, C. Guillou, E. Maccioni, F. Reniero, Photolysis of α-tocopherol in olive oils and model systems, J. Agric. Food Chem. 46 (1998) 4529–4533.
[12] K.A. Kramer, D.C. Liebler, UVB induced photooxidation of vitamin E, Chem. Res. Toxicol. 10 (1997) 219–224.
[13] T. Miyazawa, T. Yamashita, K. Fujimoto, Chemiluminescence detection of 8a hydroperoxy-tocopherone in photooxidized α-tocopherol, Lipids 27 (1992) 289–294.
[14] G.W. Grams, K. Eskins, G.E. Inglett, Dye-sensitized photooxidation of α-tocopherol, J. Am. Chem. Soc. 94 (1972) 866–868.
[15] Y. Zhang, Y.A. Yousef, H. Li, T.B. Melø, K. Razi Naqvi, Comparison of the photochemical behaviors of α-tocopherol and its acetate in organic and aqueous micellar solutions, J. Phys. Chem. A 115 (2011) 8242–8247.
[16] E.S. Krol, D.D. Escalante, D.C. Liebler, Mechanisms of dimer and trimer formation from ultraviolet-irradiated α-tocopherol, Lipids 36 (2001) 49–55.
[17] Molecular Descriptors Guide, Version 1.0.2, U.S Envionmental Protection Agency, https://www.epa.gov/chemical-research/toxicity-estimation-software-tool-test, last accessed July 26 2017.
[18] ISO, Water Quality. Freshwater Algal Growth Inhibition Test with Unicellular Green Algae, International Organization for Satndardization, Switzerland, 1998, pp. 11348–11353.
[19] J.M. Achord, C.L. Hussey, Determination of dissolved oxygen in nonaqueous electrochemical solvents, Anal. Chem. 52 (1980) 601–602.
[20] P.D. Bartlett, G.D. Mendenhall, A.P. Schaap, Competitive modes of reaction of singlet oxygen, Ann. N. Y. Acad. Sci. 171 (1970) 79–88.
[21] L.R. Gaspar, P.M. Campos, Photostability and efficacy studies of topical formulations containing UV-filters combination and vitamins A, C and E, Int. J. Pharm 343 (2007) 181–189.
[22] T. Guaratini, M.D. Gianeti, P.M. Campos, Stability of cosmetic formulations containing esters of Vitamins E and A: chemical and physical aspects, Int. J. Pharm 327 (2006) 12–16.
[23] G.H. Wheldon, A. Bhatt, P. Keller, H. Hummler, d,1-alpha-Tocopheryl acetate (vitamin E): a long term toxicity and carcinogenicity study in rats, Int. J. Vitam. Nutr. Res. 53 (1983) 287–296.
[24] H. Kappus, A.T. Diplock, Tolerance and safety of Vitamin E: a toxicological position report, Free Radic. Biol. Med. 13 (1992) 55–74.
[25] J.A. Black, W.J. Birge, A.G. Westerman, P.C. Francis, Comparative aquatic toxicology of aromatic hydrocarbons, Fundam. Appl. Toxicol. 3 (1983) 353–358.
[26] E. Gebhart, H. Wagner, K. Grziwok, H. Behnsen, The action of anticlastogens in human lymphocyte cultures and their modification by rat-liver S9 mix. II. Studies with vitamins C and E, Mutat. Res. 149 (1985) 83–94.
[27] E.B. Hook, K.M. Healy, A.M. Niles, R.G. Skalko, Vitamin E: teratogen or anti-teratogen? Lancet 1 (1974) 809.
[28] T.H. Shepard, Catalog of Teratogenic Agents, 13th ed., The Johns Hopkins University Press, Baltimore, MD, 2010, pp. 478.
[29] D.W. Cheng, T.A. Bairnson, S.A.N. Rao, S. Subbammal, Effect of variations on the incidence of teratogenicity in vitamin E-deficient rats, J. Nutr. 71 (1960) 54–60.
[30] C.E. Steele, E.H. Jeffery, A.T. Diplock, The effect of vitamin E and synthetic antioxidants on the growth in vitro of explanted rat embryos, J. Reprod. Fertil. 38 (1974) 115–123.
[31] L.S. Hurley, D.D. Dungan, C.L. Keen, B. Lönnerdal, The effects of vitamin E on zinc deficiency teratogenesis in rats, J. Nutr. 113 (1983) 1875–1877.